Supplementary Information

Structure and dynamics of γ-secretase with presenilin 2 compared to presenilin 1

Budheswar Dehury[1], Ning Tang[1], Tom L. Blundell[2], and Kasper P. Kepp[1*]

[1] *Department of Chemistry, Technical University of Denmark, DK-2800 Kongens Lyngby, Denmark*

[2] *Department of Biochemistry, University of Cambridge, Cambridge, CB2 1GA, United Kingdom*

[*]Corresponding author. E-mail: kpj@kemi.dtu.dk. Phone: +045 45252409

Tables

Table S1. A comparative analysis of model validation statistics of the homology model of PS2 (Glu77-Ile448) and the cryo-EM structure of PS1 (PDB ID: 5FN2) using various three-dimensional model evaluation servers.

Model validation Servers	Model quality parameters	Validation scores	
		PS2 homology model	**Experimental PS1 (PDB ID: 5FN2)**
Procheck	Most favored regions (%)	90.5	88.5
(Ramachandran plot)	Additional allowed regions (%)	8.3	5.4
	Generously allowed regions (%)	0.3	3.5
	Disallowed regions (%)	0.9	2.6
Richardson Lab's Molprobity	Most favored regions (%)	92.7	89.6
(Ramachandran Plot)	Allowed regions (%)	6.2	5.8
	Disallowed regions	1.1	4.6
Errat	Overall quality (%)	80.3	80.8
ProSA	Z score	-3.45	-3.19
ProQ	LG score	2.21	3.67
	Max Sub	0.12	0.36
Prove	Z score mean	0.48	0.21
METAMQAPII	GDT_TS	49.6	48.2
	RMSD	3.7	3.2

Table S2. Variation in distances between amino acids used for subdomain distance measurements and angle calculations. The last 300 ns trajectories of the three PS2 γ-Secretase systems were used for calculation.

Simulations	Distance			Angle
	Val328-Asp263	Leu121-Asp263	Leu121-Val328	Val328-Leu121-Asp263
Simulation 1	7.22 + 0.01	6.32 + 0.97	3.92 + 0.03	60. 95 + 1.27
Simulation 2	7.43 + 0.11	6.19 + 0.08	3.96 + 0.04	56.37 + 1.18
Simulation 3	7.13 + 0.22	6.54 + 0.16	3.95 + 0.03	65. 48 + 1.98

Val328 is located within the large lobe of Nicastrin, and Leu121 is in the small lobe of Nicastrin. Asp263 is one of the two catalytic residues of Presenilin 2.

Figures

```
              1        10        20        30        40        50        60        70        80        90
PSN1_HUMAN  .....MTELPAPLSYFQNAQMSEDNHLSNTVRSQNDNRERQEHNDR.RSLGHPEPLSNGRPQGNSRQVVEQDEEEDEELTLKYGAKHVIMLFVPVTLCMV
PSN2_HUMAN  MLTFMASDSEEEVCDERTSLMSAESPTPRSCQEGRQGPEDGENTAQWRSQENEEDGEEDPDRYVCSGVPGRPPGLEEELTLKYGAKHVIMLFVPVTLCMI
              100       110       120       130       140       150       160       170       180       190
PSN1_HUMAN  VVVATIKSVSFYTRKDGQLIYTPFTEDTETVGQRALHSILNAAIMISVIVVMTILLVVLYKYRCYKVIHAWLIISSLLLLFFSFIYLGEVFKTYNVAVD
PSN2_HUMAN  VVVATIKSVRFYTEKNGQLIYTPFTEDTPSVGQRLLNSVLNTLIMISVIVVMTIFLVVLYKYRCYKFIHGWLIMSSLMLFLFTYIYLGEVLKTYNVAMD
              200       210       220       230       240       250       260       270       280       290
PSN1_HUMAN  YITVALLIWNFGVVGMISIHWKGPLRLQQAYLIMISALMALVFIKYLPEWTAWLILAVISVYDLVAVLCPKGPLRMLVETAQERNETLFPALIYSSTMVW
PSN2_HUMAN  YPTLLLTVWNFGAVGMVCIHWKGPLVLQQAYLIMISALMALVFIKYLPEWSAWVILGAISVYDLVAVLCPKGPLRMLVETAQERNEPIFPALIYSSAMVW
              300       310       320       330       340       350       360       370       380       390
PSN1_HUMAN  LVNMAEGDPEAQRRVSKNSKYNAESTERESQDTVAENDDGGFSEEWEAQRDSHLGPHRSTPESRAAVQELSSSILAGEDPEERGVKLGLGDFIFYSVLVG
PSN2_HUMAN  TVGMAKLDPSSQGALQL..PYDPEM.EEDSYDSFGEPS...YPEVFEPPLTGYPG............EEL.......EEEEERGVKLGLGDFIFYSVLVG
              400       410       420       430       440       450       460
PSN1_HUMAN  KASATASGDWNTTIACFVAILIGLCLTLLLLAIFKKALPALPISITFGLVFYFATDYLVQPFMDQLAFHQFYI
PSN2_HUMAN  KAAATGSGDWNTTLACFVAILIGLCLTLLLLAVFKKALPALPISITFGLIFYFSTDNLVRPFMDTLASHQLYI
```

Figure S1. Pair-wise sequence alignment of PS1 and PS2 using MultAlin and rendered through ESPript. Similar amino acids are highlighted in boxes, and completely conserved residues are indicated by white lettering on a red background. The two conserved catalytic aspartates i.e., Asp-257/Asp-263 and Asp-385/Asp-366 (of PS1 and PS2), are highlighted using red stars.
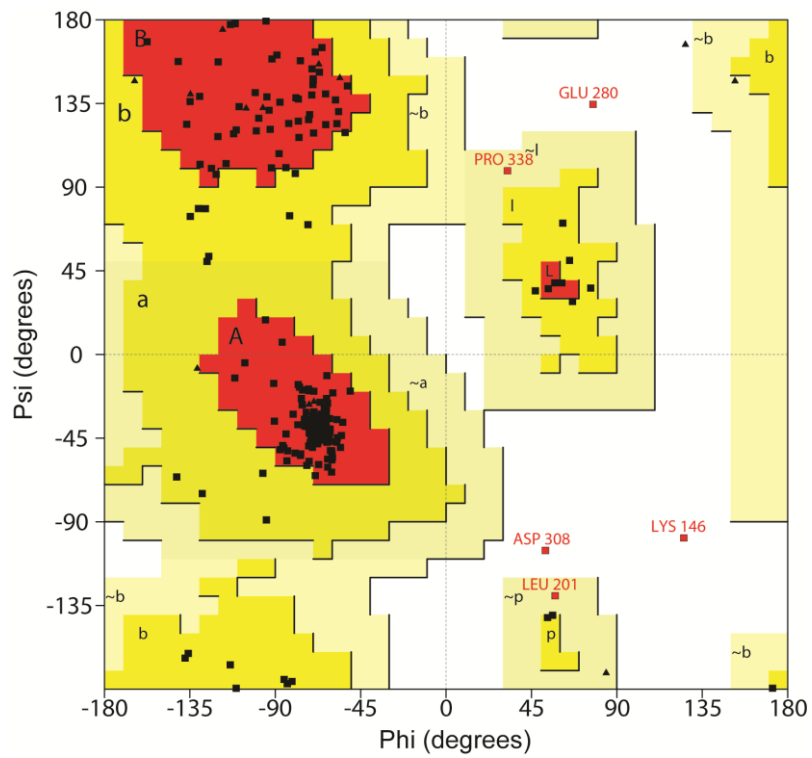
Figure S2. Ramachandran plot of the homology modeled PS2 displaying the phi (φ) and psi (ψ) distribution of amino acids, obtained using PROCHECK.
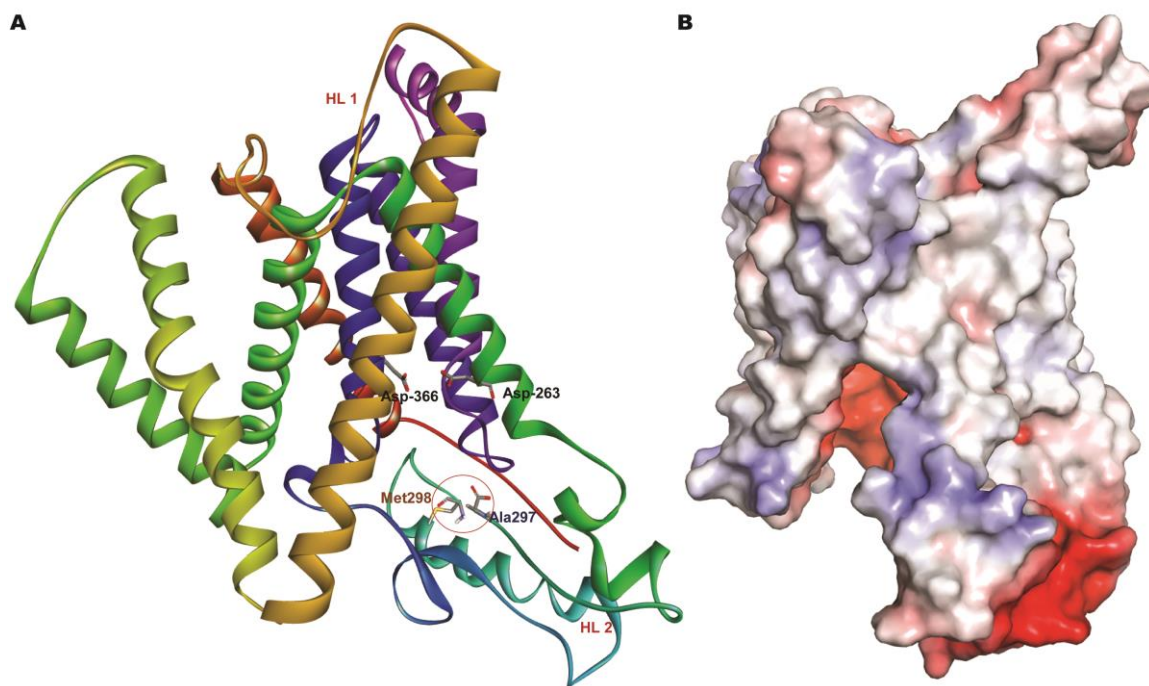
Figure S3. The mature form of PS2 with N-terminal fragment (CTF) and C-terminal fragment (CTF) after cleavage of the peptide bond between Ala-297 and Met-298 (**A**). (**B**) The electrostatic surface potential of the modeled PS2 calculated using the APBS plugin of PyMOL version 2.2 (Schrödinger, LLC). The negative surface potential is shown in red color and positive potential is shown in blue surface color.
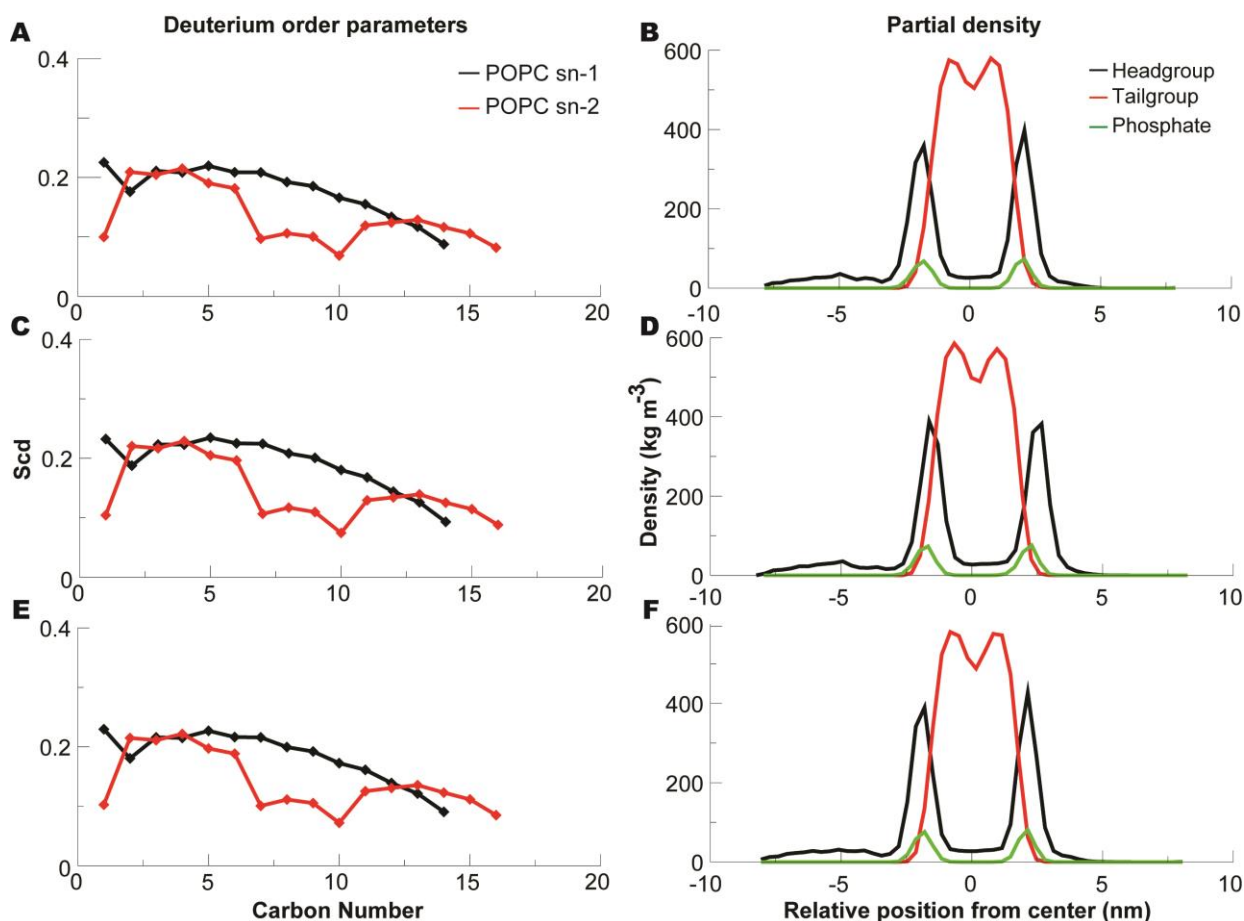
Figure S4. The lipid order parameters, i.e., deuterium order of acyl chains and density profiles of POPC lipid bilayer averaged over the 500 ns of MD of PS2 γ-Secretase. (**A**) The acyl chain order parameter distributions of Sn-1 (black) and sn-2 (red) of the POPC lipid bilayer of simulation 1. (**B**) The density profile of lipid headgroups, tailgroups, and phosphate of POPC bilayer from simulation 1. (**C**) The acyl chain order parameter distributions of Sn-1 (black) and sn-2 (red) of the POPC lipid bilayer of simulation 2. (**D**) The density profile of lipid headgroups, tailgroups, and phosphate of POPC bilayer from simulation 2. (**E**) The acyl chain order parameter distributions of Sn-1 (black) and sn-2 (red) of the POPC lipid bilayer of simulation 3. (**F**) The density profile of lipid headgroups, tailgroups, and phosphate of POPC bilayer from simulation 3.
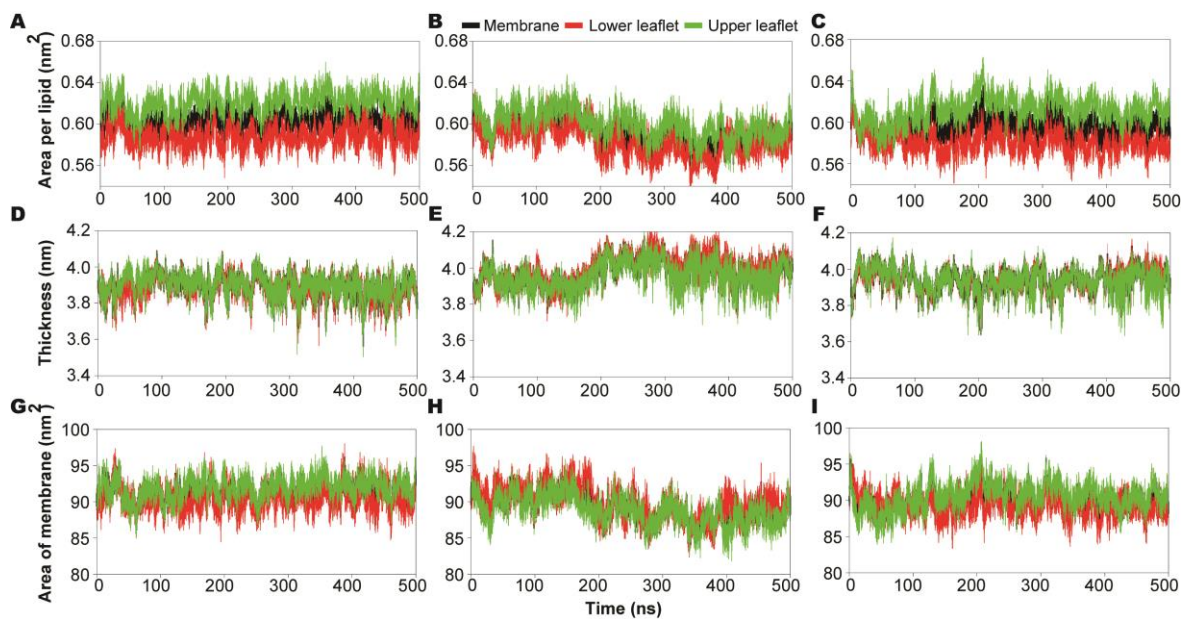
Figure S5. Membrane quality control validated by area per lipid, membrane thickness, and area of the membrane (the membrane is shown in black, the lower leaflet is red, and the upper leaflet is green) during the full 500 ns of MD for all three independent simulations. (**A-C**) The area per lipid parameter of POPC bilayer from simulation 1 (A), simulation 2 (B), and simulation 3 (C). (**D-F**) Bilayer thicknesses from simulation 1 (D), 2 (E), and 3 (F). (**G-I**) The computed area of the membrane in the total simulated membrane-protein system from simulation 1 (G), 2 (H), and 3 (I).
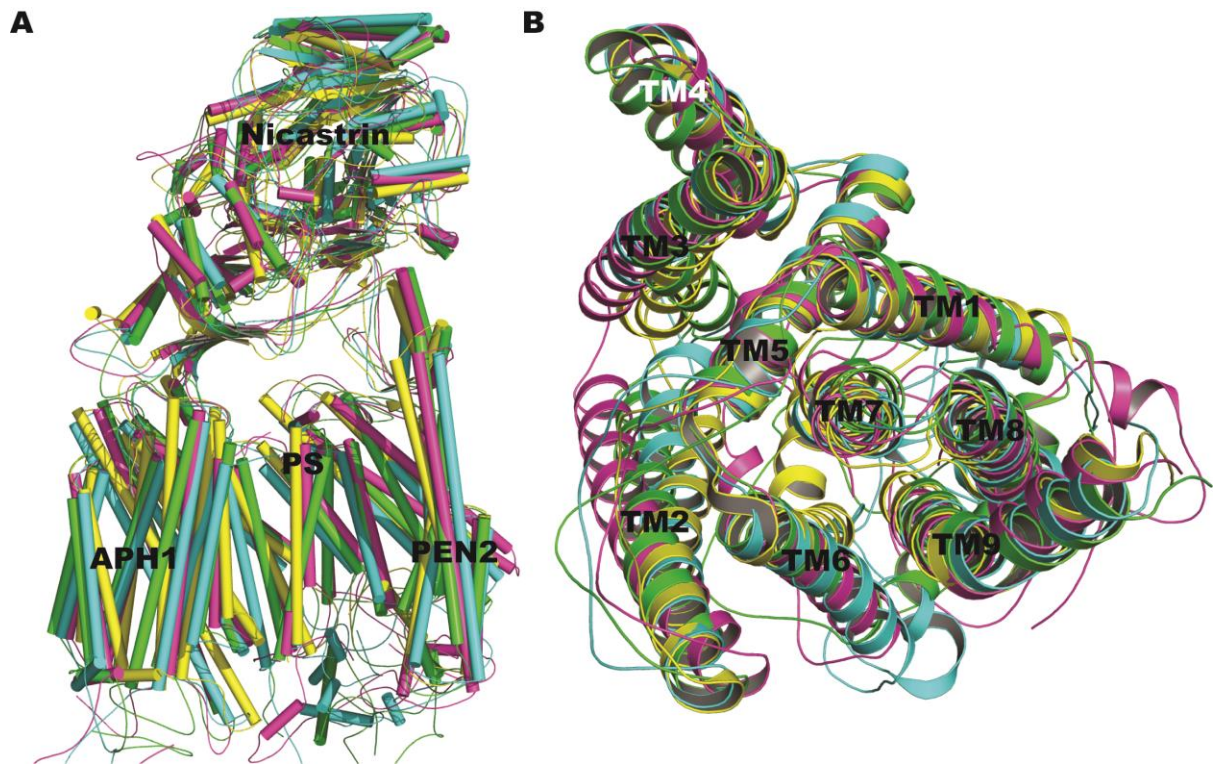
Figure S6. (A) Structural superposition of representative structures of PS2-γ-secretase with the cryoEM structure PS1-γ-secretase (5FN2) obtained using PyMOL**. (B)** Structural superimposition of PS2 representative structures after MD and the PS1 subunit from the cryo-EM structure 5FN2 (green: representative structure obtained from simulation 1; cyan: structure from simulation 2; magenta: structure from simulation 3; yellow: cryoEM structure 5FN2). Structural superposition was based on the Cα-atom pairs.
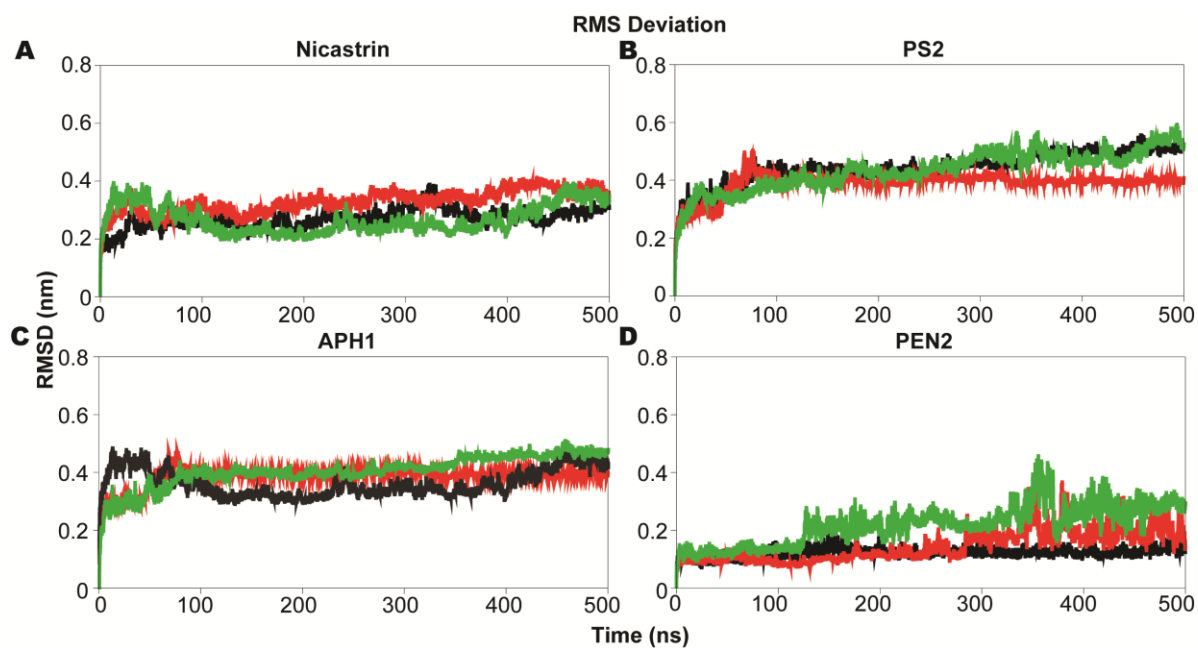
Figure S7. The intrinsic dynamic stability showing the backbone root mean squared deviation (RMSD) of the four subunits Nicastrin (**A**), PS2 (**B**), APH1 (**C**) and PEN2 (**D**) of PS2-γ-secretase over 500 ns from three independent simulations (simulation 1: black, simulation 2: red and simulation 3: green).
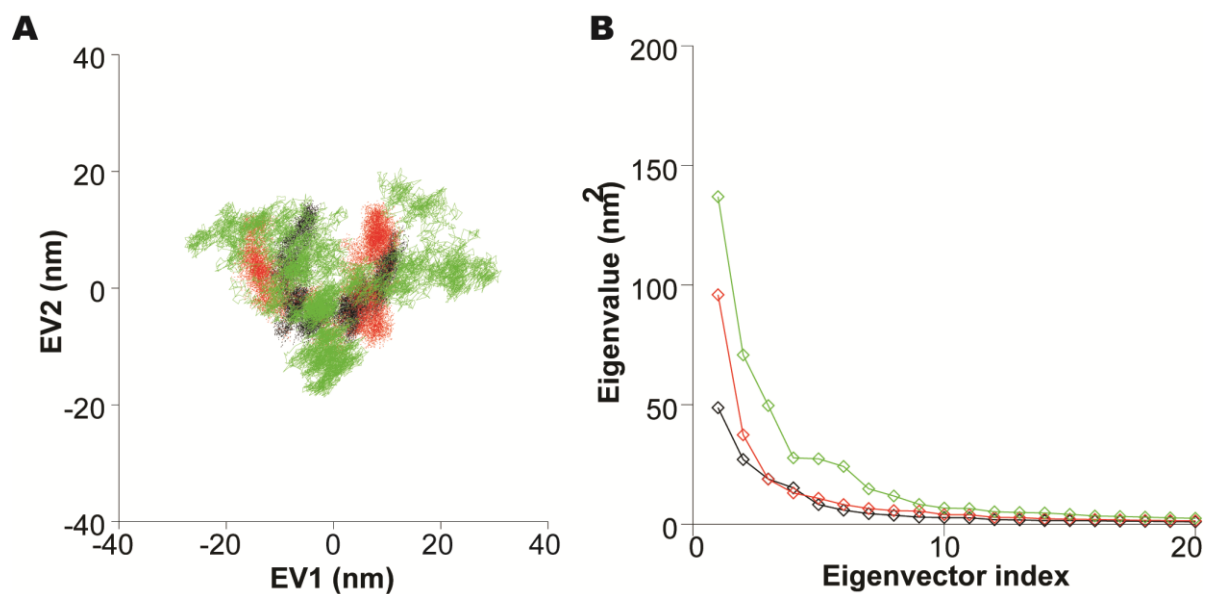
Figure S8. Principal component analysis of main-chain atoms of PS2 γ-secretase. (**A**) The 2D projection trajectories in phase space displaying the top-two eigenvectors EV1 and EV2. Simulation 1 occupied least space, while simulation 3 acquired more space due to movement. (**B**) The movement of main-chain atoms on the basis of eigenvalues. The analysis was performed using the last 300 ns of each simulation (black: Simulation 1, red: Simulation 2 and green: Simulation 3).
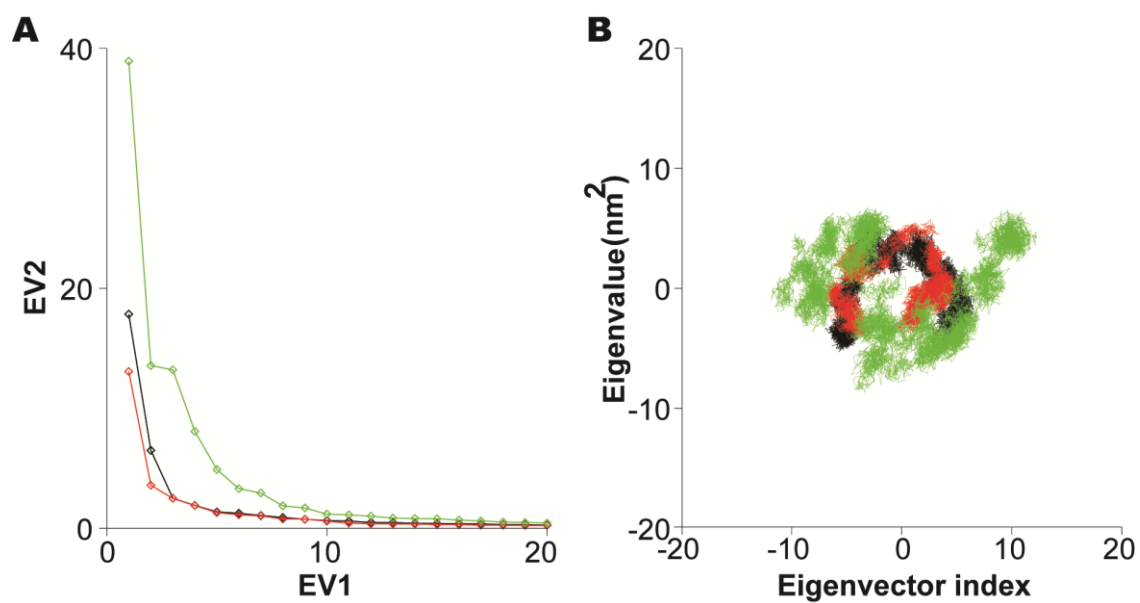
Figure S9. Principle-component analysis of main-chain atoms of PS2 extractied frin the full structure of the last 300 ns of each of the three independent simulations of PS2-γ-secretase in POPC. (**A**) The movement of main chain atoms of PS2 on the basis of eigenvalues (black: Simulation 1, red: Simulation 2 and green: Simulation 3). (**B**) The 2D projection of EV1 and EV2 in phase space.
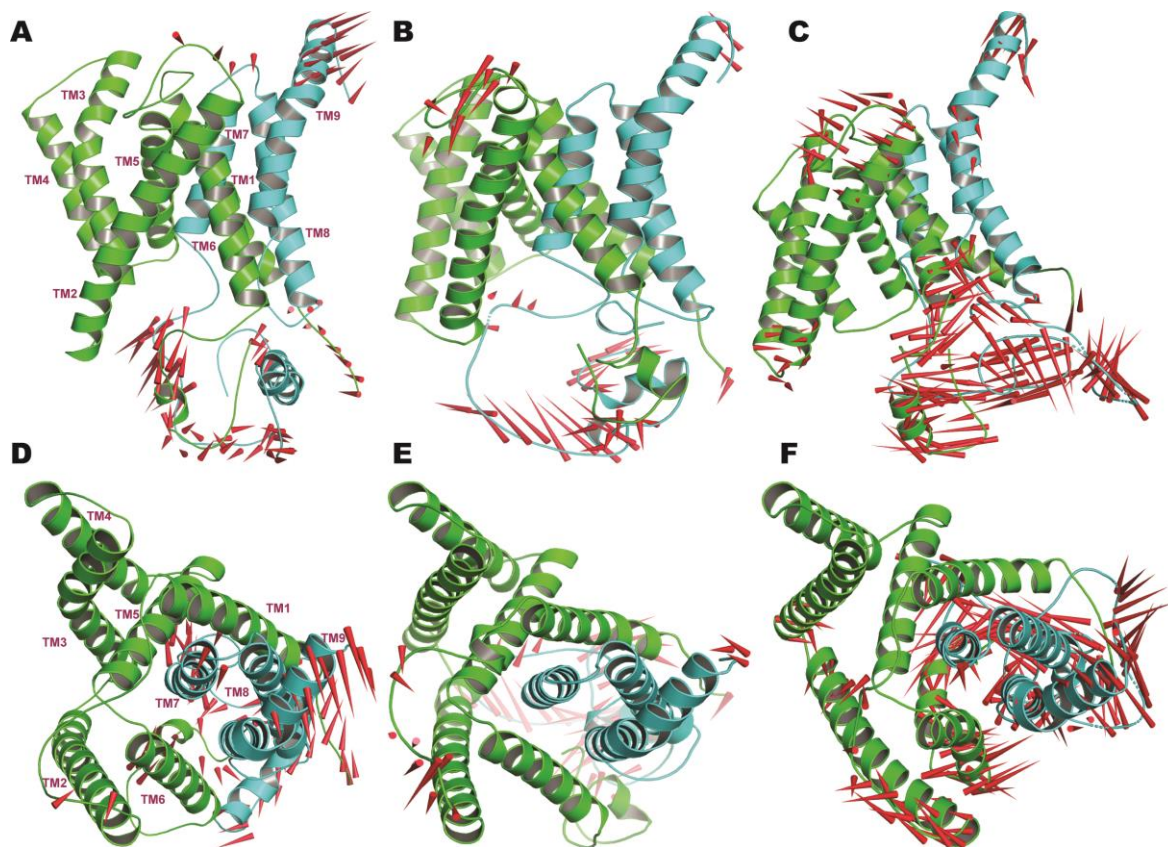
Figure S10. Porcupine plots displaying the main motions of PS2 alone extracted from the top one eigenvector (EV1) from the last 300 ns of the trajectory of three independent simulation of PS2-γ-Secretase. Panels **A-C** show the movement of the nine TM helices and their loops of PS2 for Simulation 1 (A), 2, (B), and 3 (C), and **D-F** display the corresponding rotated top views. The arrows represent the direction of motion and the lengths depict the amplitude of motion (the NTF and CTF are shown in green and cyan, respectively). HL2, TM2, and TM9 show particular movements in simulation 3 representating the loose conformation state.
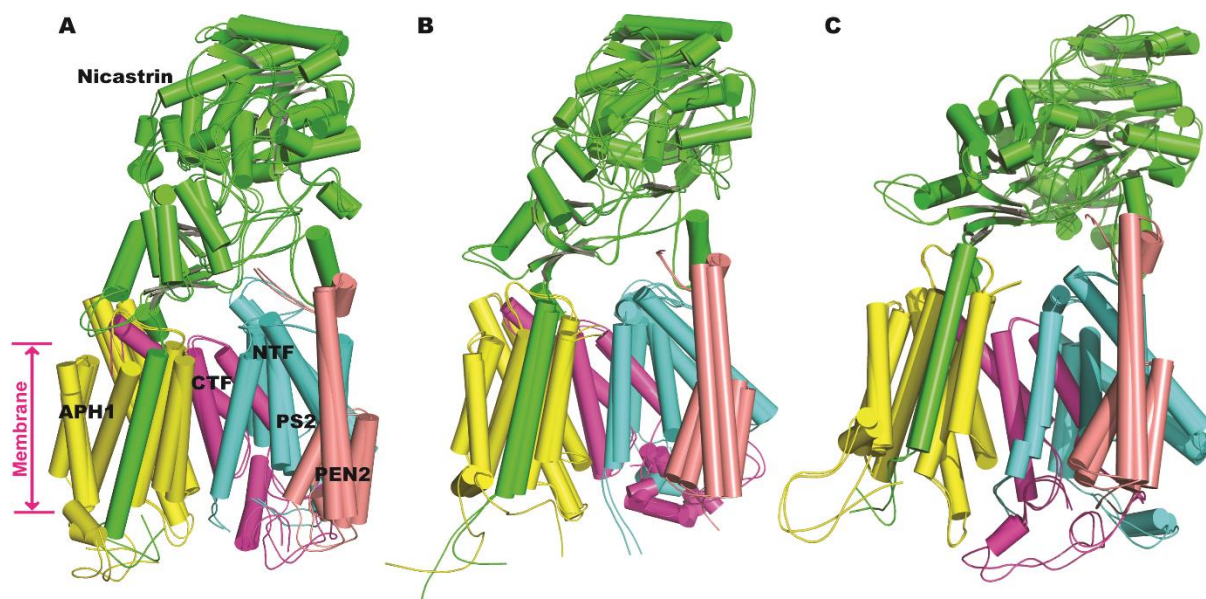
Figure S11. Structural superimposition of the top-two representative structures of PS2-γ-secretase colored by subunit (Nicastrin: Green, PS2-NTF: Cyan, PS2-CTF: Magenta, APH1: Yellow, and PEN2: Tint wheat) from the three simulations obtained by clustering analayis using the Gromos method. (**A**) Structural superposition of the two most representative structures of PS2-γ-secretase from simulation 1. (**B**) Structural superposition of the two most representative structures from simulation 2. (**C**) Structural superposition of the two most representative structures from simulation 3.
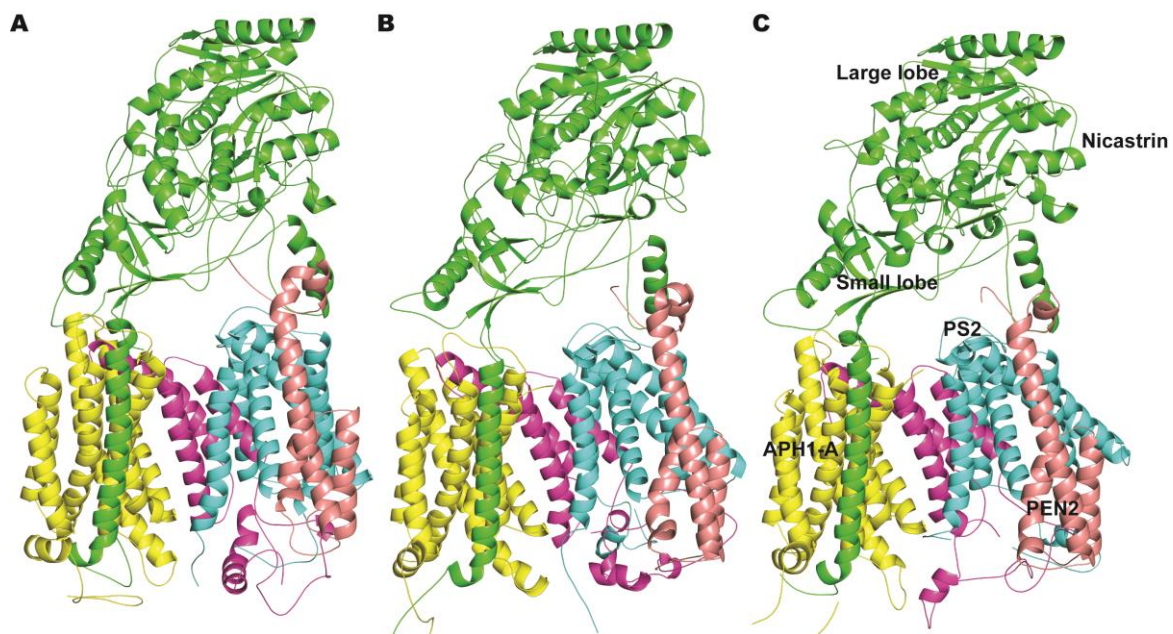
Figure S12. Representative structures of PS2-γ-secretase colored by subunit (Nicastrin: Green, PS2-NTF: Cyan, PS2-CTF: Magenta, APH1-A: Yellow, and PEN2: Tint wheat) from the three simulations obtained by clustering using the Jarvis-Patrick algorithm. **A**: Representative structure of PS2-γ-secretase from simulation 1, **B:** Representative structure from simulation 2 and **C:** Representative structure from simulation 3.
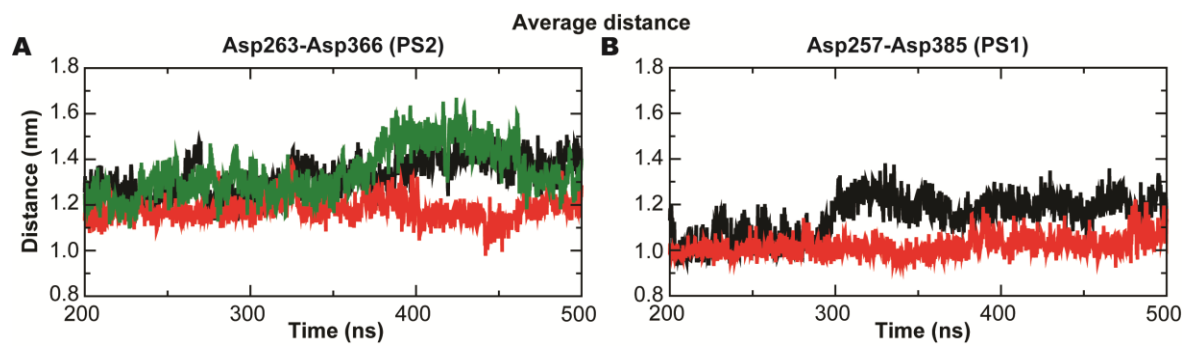
Figure S13. The average distance profile of the catalytic pairs of PS2 (**A**) and PS1 γ-secretase (**B**) systems in POPC lipid bilayer during the last 300 ns of simulation (Black: Simulation 1, Red: Simulation 2 and Green: Simulation 3).
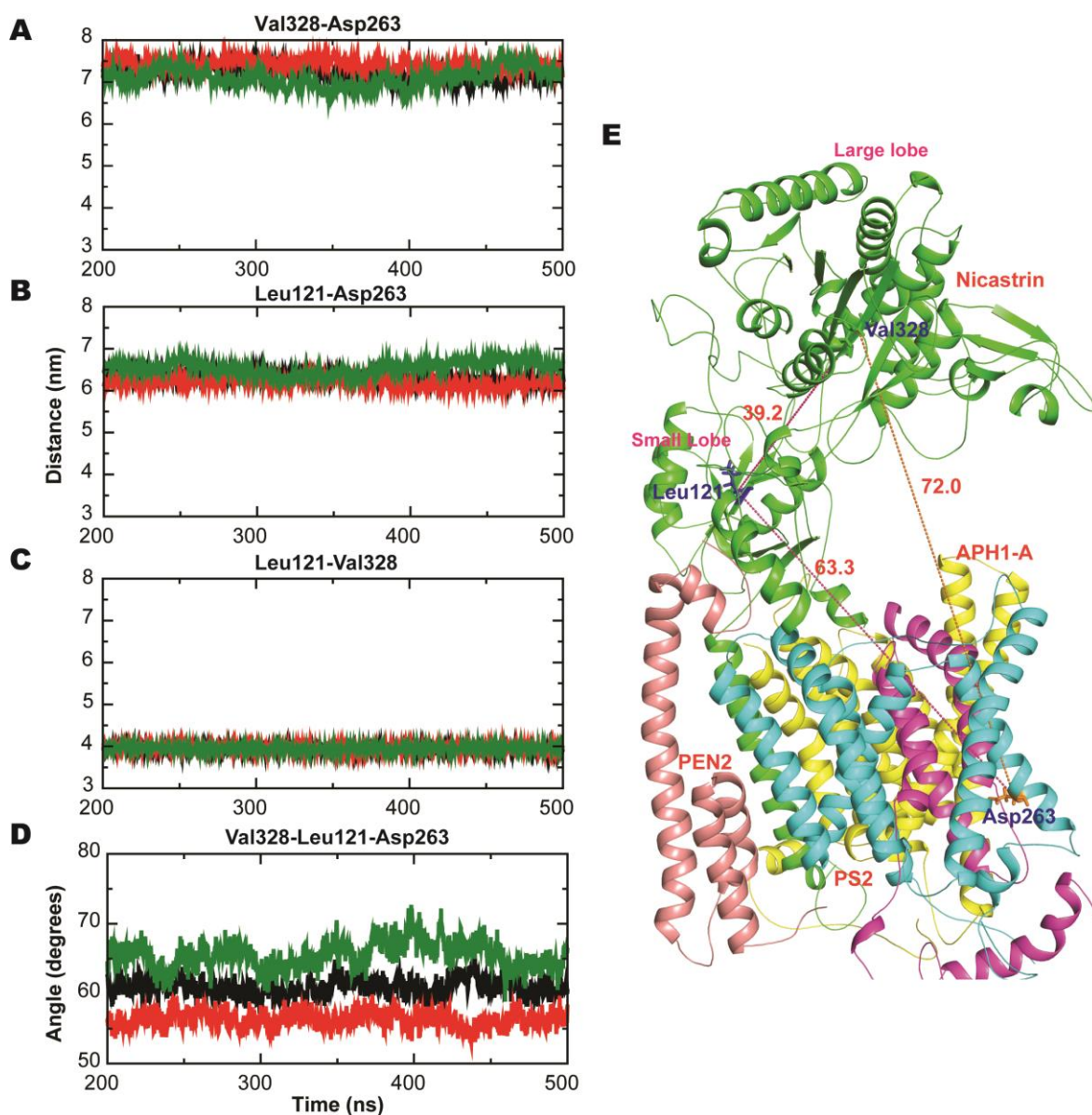
Figure S14. Distance and angle variations of key amino acids measured during the last 300 ns of simulation. (**A**) Distance between Val328 located within the large lobe and the catalytically active aspartate Asp263 (located in TM6) of PS2. (**B**) Distance between Leu121 of the small lobe and Asp263 of PS2. (**C**) Distance between the two ECD lobes (Leu121 and Val328). (**D**) Angle between Val328, Leu121, and Asp263. (**E**) A snapshot (obtained from the top ranked cluster structure of simulation 1) of PS2-γ-secretase displaying key distances between amino acids of the NCT ECD and the catalytic aspartate.
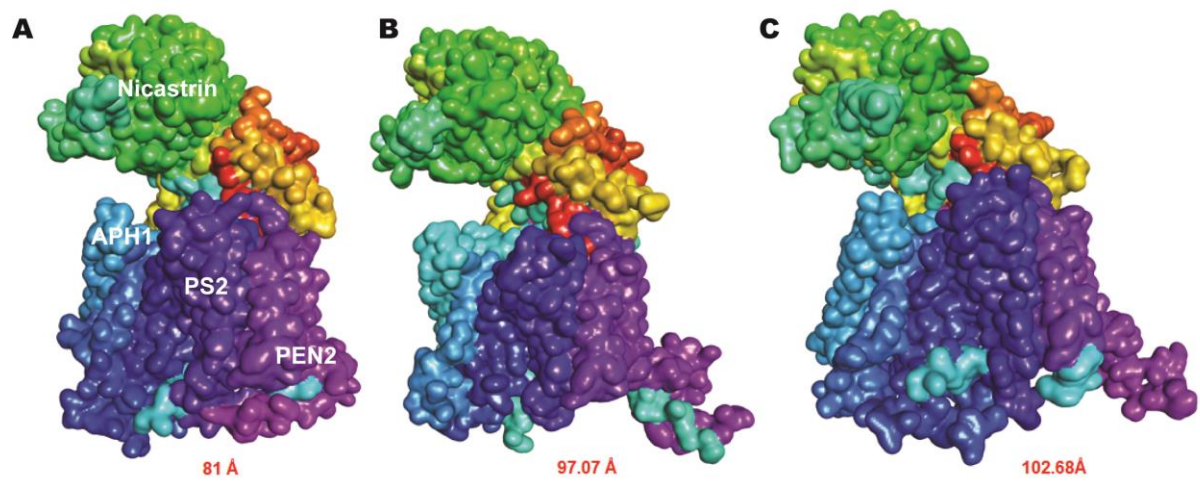
**Figure S15.** The surface representation of the compact, intermediate, and loose conformations of PS2-γ-secretase obtained by cluster analysis of the last 300 ns (the bottom length was computed as the horizontal maximal extension using VMD). Simulation 3 depicts a looser state that takes up more space in the membrane.
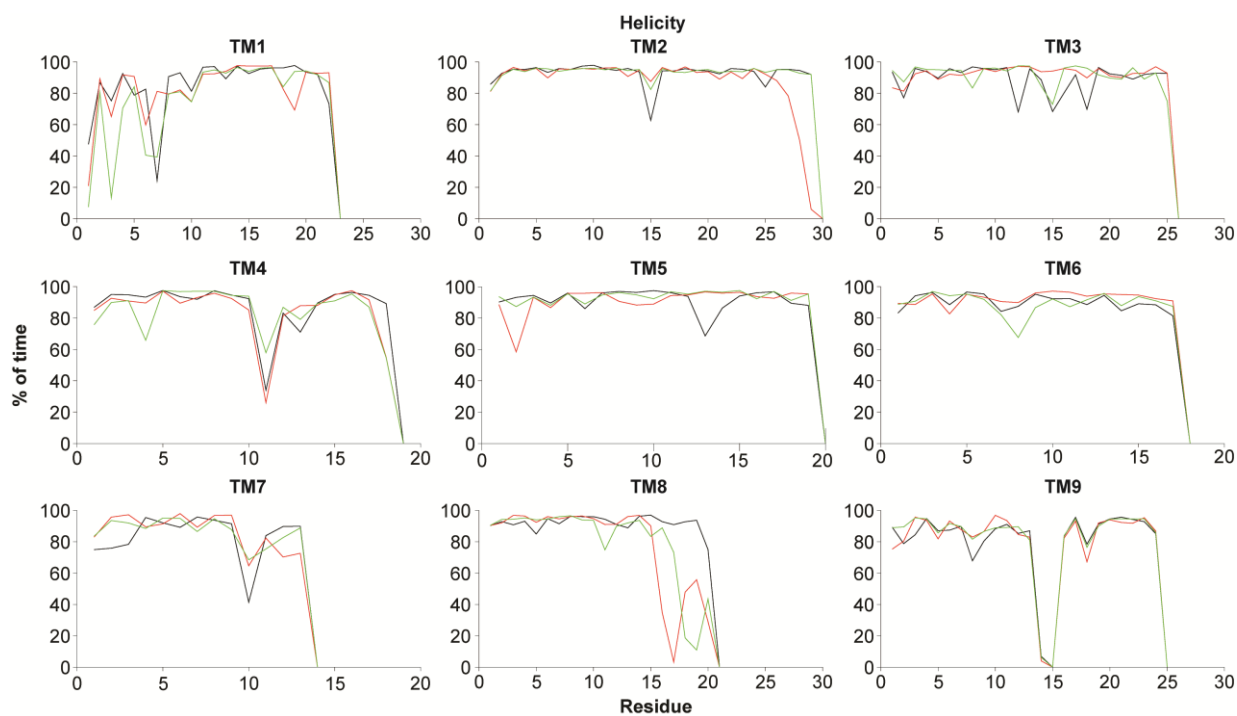
Figure S16. Retention of helical properties measured in terms of helicity of all TMs of PS2 during the last 300 ns of all-atoms MD simulation of PS2 γ-secretase. The helical properties of each TM was computed using the *gmx helix* utility program of GROMACS.
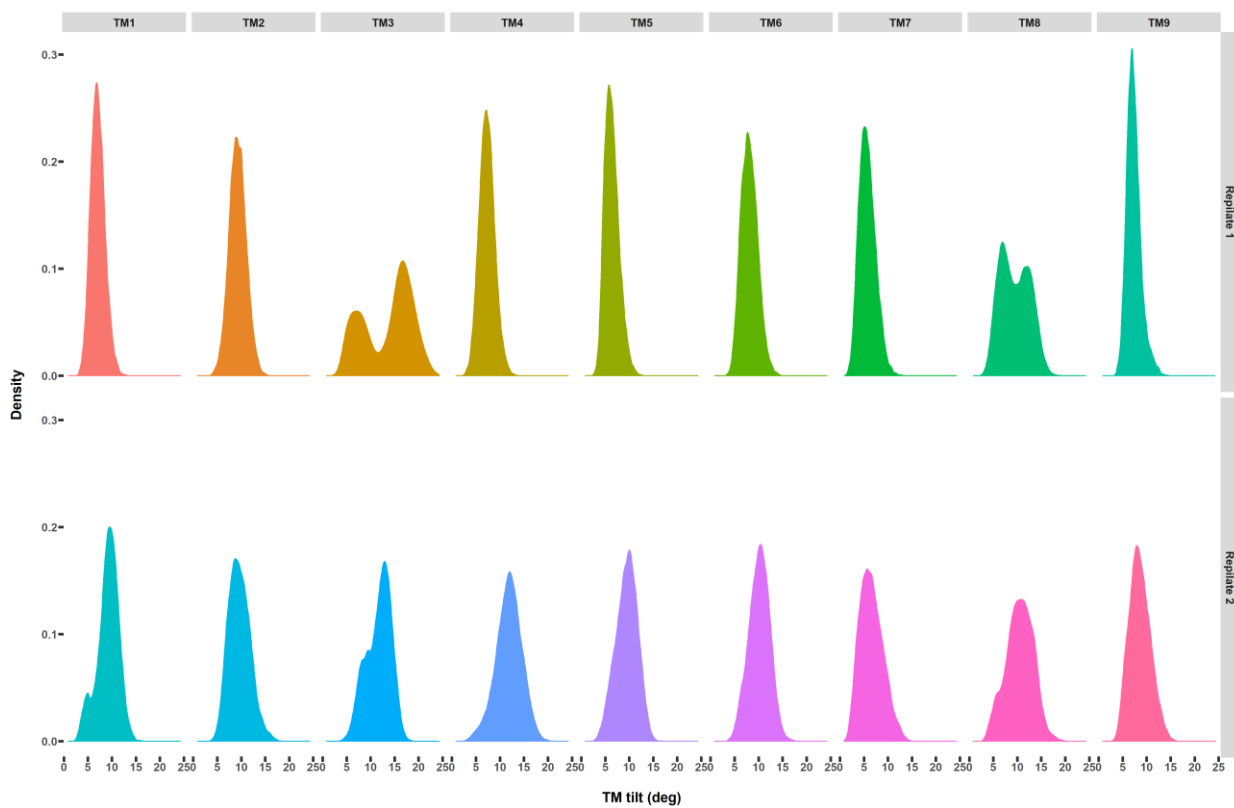
Figure S17. The density profile of the distribution of tilt angles of each TM of PS1 calculated from the last 300 ns of the trajectory (two independent simulations) of PS1-γ-secretase in POPC lipid bilayer.
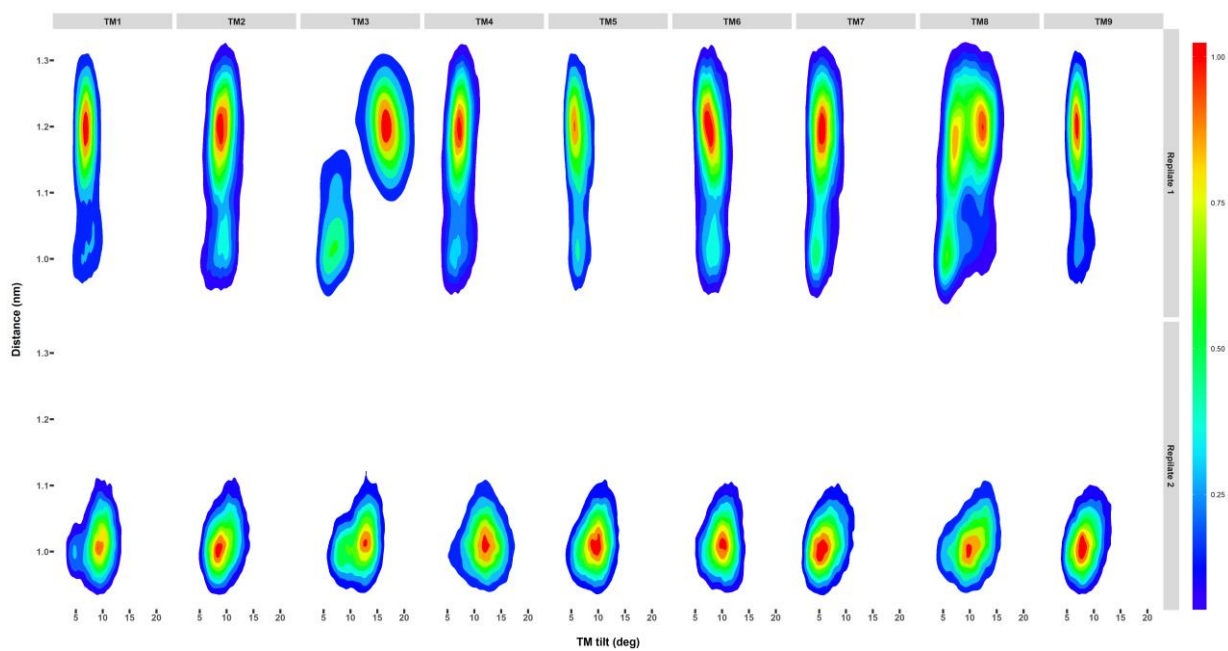
Figure S18. The distribution of snapshots, when projected onto the distance between the catalytic pairs (Asp-257 and Asp-385) and computed tilt angles of each TM of PS1-γ-secretase during the last 300 ns of MD simulation of two independent simulations in pure POPC lipid bilayer. The colored scale defines the relative populations.
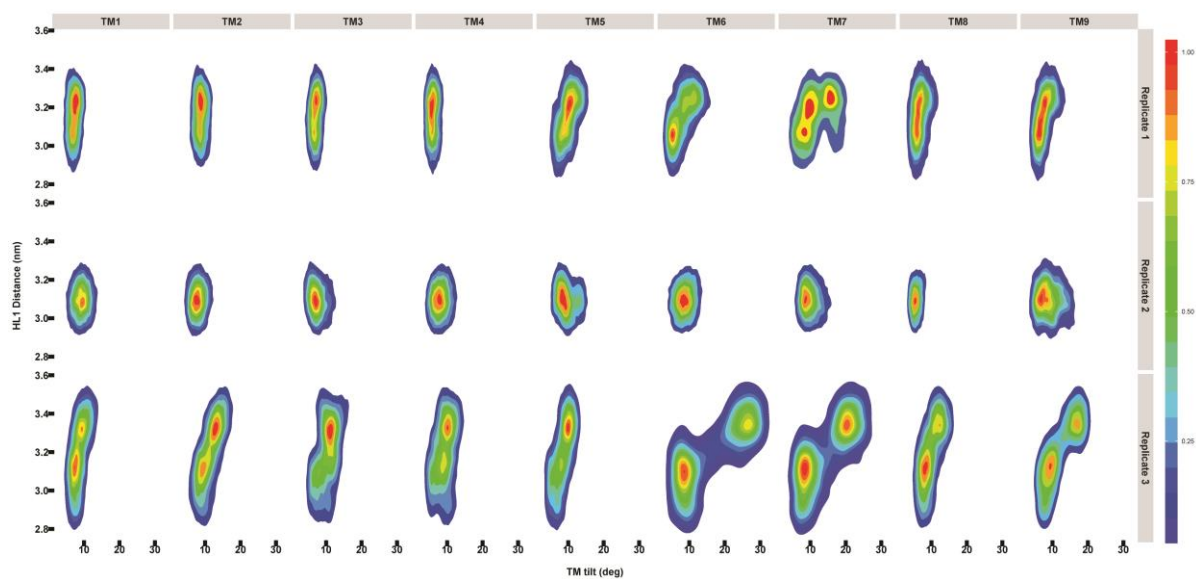
Figure S19. The distribution of snapshots projected onto the distance between the residues at the distal ends of HL1 (Val-109 and Ser-130) and tilt angles of TM helices of PS2 for the three independent simulations in pure POPC lipid bilayer. The colored scale defines the relative populations. Strong correlations are seen in particular in the loose state (bottom row, Simulation 3) between the TM6, TM7, and TM9 tilts and the HL1 distance.
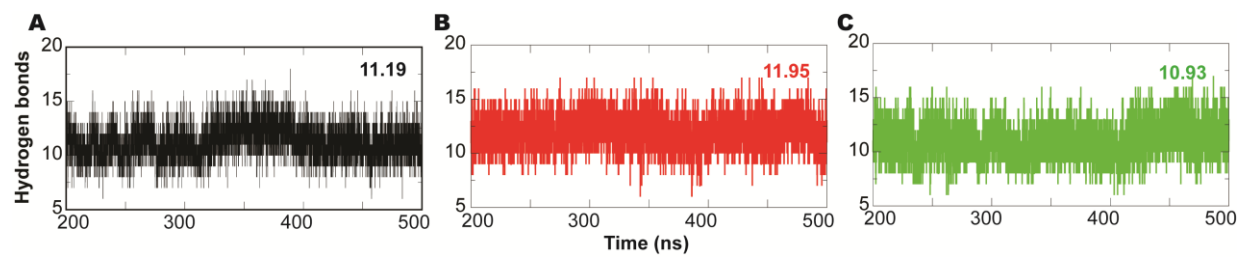
Figure S20. Number of hydrogen bonds between the catalytic Asp-263 and Asp-366 of PS2 and water molecules during the last 300 ns MD simulations (A:simulation 1, B:simulation 2, and C: simulation 3.
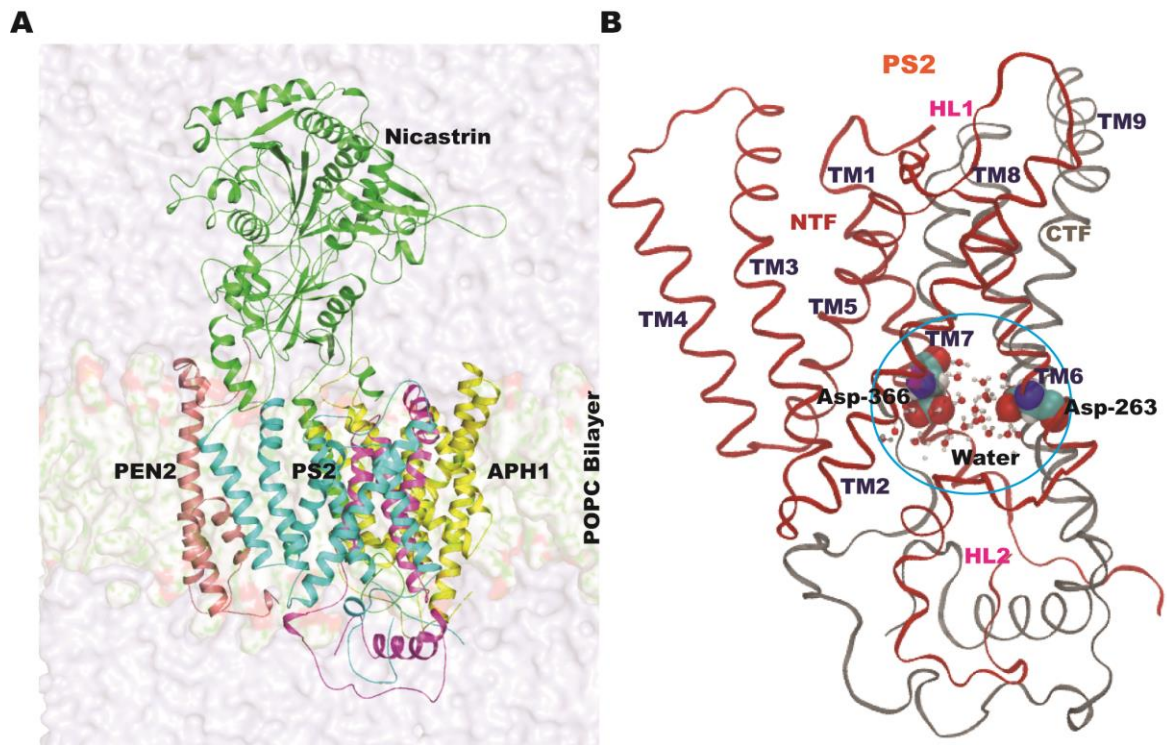
Figure S21. (A) Snapshot showing the position of different subunits within the lipid bilayer. **(B)** Solid ribbon representation of PS2 along with prominent water molecules (shown in ball and stick format) that are accessible to the catalytic site (within 4 Å).